The Open Biomedical Engineering Journal

Content list available at: https://openbiomedicalengineeringjournal.com

CrossMark

RESEARCH ARTICLE

Complete Unsteady One-Dimensional Model of the Net Aortic Pressure Drop

Francesca M. Susin[1,*]

[1]*Cardiovascular Fluid Dynamics Laboratory (HER Lab) - Department of Civil, Environmental and Architectural Engineering (DICEA), University of Padova, via Marzolo 9, I-35131 PADOVA, Italy*

Abstract:

Background:

A large amount of engineering and medical research has been devoted to the assessment of aortic valve stenosis severity in the past decades. The net transvalvular pressure drop has been recognized as one of the parameters that better reflect stenosis effects on left ventricle overload, and its adoption in clinical assessment of stenosis has been proposed. Flow unsteadiness has been shown to have a non-negligible impact on the net drop; however, a simple formulation for net drop calculation that includes not only flow pulsatility but also the effects of valve dynamics is still lacking.

Objective:

The present contribution is hence aimed at developing a *complete unsteady* one-dimensional model of the net aortic transvalvular pressure drop that just requires non-invasive data to be implemented.

Methods:

Transvalvular flow is described as a jet of incompressible viscous fluid through a circular orifice placed in a concentric rigid circular tube. The classical one-dimensional mass and total head conservation equations are applied. The effective orifice area and transvalvular flow rate are assumed to vary with time throughout the ejection period.

Results:

The model is found to capture pressure drop oscillations occurring when the valve opens/closes and/or leaflets flutter, thanks to the inclusion of valve dynamics effects. The model is also proposed as a numerical tool for the calculation of the instantaneous effective orifice area once net pressure drop and flow rate are known.

Conclusion:

The model may contribute to the improvement of non-invasive aortic stenosis assessment.

Keywords: Aortic valve stenosis, Net pressure drop, Valve dynamics, Effective orifice area, Unsteady flow, Analytical model, Non-invasive assessment.

1. INTRODUCTION

Clinical non-invasive assessment of heart valves hemo-dynamics and *in-vitro* assessment of prosthetic valves performance are fundamental issues widely investigated in the literature in the past decades. The unanimous objective is the development of reliable tools that can help clinicians in the diagnosis and therapy of valvular diseases [1 - 8], and support the development of safe and effective heart valve substitutes [9 - 13].

Native aortic valve stenosis (AS) is the most common valvular disease in the western countries, and its incidence is destined to increase due to the aging population. It is a pathologic state characterized by a valvular orifice area smaller than the healthy one. Blood ejected from the left ventricle through the narrowed orifice experiences a sort of obstruction, and is affected by pressure loss due to turbulence just downstream of the valve. The left ventricle is hence forced to work against an increased afterload. AS can be either congenital or acquired. In the first case, bicuspid aortic valve is the most frequent valvular anomaly that leads to stenosis, in infancy or later in time [14]. In the second case, the usual degenerative process is a progressive calcification of valvular leaflets [15]. Whatever the etiology, management of stenotic

* Address correspondence to this author at the Cardiovascular Fluid Dynamics Laboratory (HER Lab) - Department of Civil, Environmental and Architectural Engineering (DICEA), University of Padova, via Marzolo 9, I-35131 PADOVA, Italy; Tel: +39 49 8275443; Fax: +39 49 8275446; E-mail: francescamaria.susin@unipd.it

patients is of great importance since progression of the disease, whether untreated, is fatal [5]. Accurate assessment of stenotic lesion gravity is then crucial for patient treatment and for the selection of the appropriate timing for surgical or transcatheter valve replacement [3]. Graduation of the pathology by comparison of estimated values to reference cutoff given in international guidelines [16] usually proves effective for the majority of patients. Nevertheless, the debate around the improvement of assessment of aortic stenosis is far from being concluded yet, as demonstrated by recent comprehensive reviews on the topic [3, 5, 17]. This is mainly due to the complexity of both the pathology, often coupled to commorbidities, and valvular solid and flow mechanics. We refer to the above reviews for a detailed panorama of possible inconsistencies between guidelines and improved diagnostics, and a description of related parameters. Here, we are interested in recalling that one of the hemodynamic indexes currently adopted to grade the severity of the stenotic lesion is the *maximum* transvalvular pressure drop Δp_{max} [5, 16, 18]. Indeed, it has been demonstrated that the pressure difference that better reflects the increased ventricular workload in aortic stenosis is the *net* transvalvular drop Δp_{net} [19, 20], which has been suggested as a possible better index of stenosis severity [4, 21]. Moreover, it has been widely recognized that inconsistencies in the graduation of stenosis severity when obtained from Doppler and catheterization, respectively, can be mainly ascribed to the fact that Doppler measurements estimate Δp_{max} while catheterization usually measures Δp_{net} [3].

Some theoretical models have been proposed in the literature to predict the instantaneous pressure difference across both native and prosthetic aortic valves [19, 22 - 25]. In particular, Garcia and co-authors have derived a simple and effective analytical expression for Δp_{net} that can be implemented with Doppler echocardiographic measurements [19]. Their theoretical approach accounted for transvalvular pulsatile flow rate and assumed constant effective orifice area during the ejection period. The extensive series of experiments performed with either *rigid* orifice plates or bioprosthetic valves (*i.e. flexible* orifices) proved the capability of the model to reliably reproduce the measured net pressure drop. However, some difference between predicted and measured Δp_{net} can be appreciated in the early systole of bioprosthetic *in-vitro* tests due to the presence of pressure drop oscillations and related peak, suggesting that valve dynamics may affect the behaviour of the instantaneous net pressure drop. As far as aortic valve dynamics is concerned, it is widely recognized that normal native and well-functioning prosthetic valves usually open and close very rapidly, and fairly stay at maximal opening during most of the systolic period [26 - 32]. On the contrary, stenotic valves not only exhibit a smaller geometric and effective orifice area at maximal opening, but also open and close more slowly [26 - 33]. In that case, the assumption of constant area during the systole to estimate the transvalvular net pressure difference might deserve some further investigation.

Following the above observations, the present study is aimed at extending the approach proposed by Garcia and colleagues [19] to develop a simple model of transvalvular flow that includes inertia terms associated not only with flow pulsatility but also with valve area unsteadiness. The theoretical analysis is detailed in Section 2, together with the description of numerical tests performed for model validation. Section 3 describes the results, which are then discussed and commented on in Section 4. Finally, Section 5 is devoted to some conclusion.

2. MATERIALS AND METHODS

2.1. Background

The instantaneous flow pattern across a stenotic aortic valve during systolic ejection is usually modelled as a jet through a circular orifice placed in a concentric circular tube that mimics the anatomical district between the left ventricle outflow tract and the ascending aorta [18, 19, 34 - 36]. The configuration of the jet through the orifice is sketched in Fig. (**1**), with the adopted notations. In order to pass the stenotic obstruction, the approaching flow contracts from some distance upstream the orifice (location 1, Fig. **1**) up to the vena contracta, the so called Effective Orifice Area (EOA), *i.e.* the smaller area of the transvalvular jet. It then expands and reattaches to the wall at some distance downstream in the aortic tube (location 2). Turbulent recirculation with a complicated eddying behaviour occurs adjacent to the jet in the expansion region and produces energy losses [37], implying a pressure drop between location 1 and location 2.

Energy dissipation is not the only mechanism that drives pressure difference between the left ventricle and the ascending aorta, but both convective and temporal acceleration of the flow also act [19, 23]. The former is related to the possible difference in the cross-sectional area of the left ventricular outflow tract and the ascending aorta, respectively. The latter is due to the unsteadiness of the flow. In the blood flow through aortic valve, not only the flow rate but also the geometrical orifice area varies in time [26, 27, 30]. As a consequence, the configuration of the whole jet through the orifice (length and cross-sectional area) varies in time as well (flow configuration at different times is depicted in Fig. **1b**). In particular, EOA dynamics typically exhibits opening, fairly constant, and closing phases with rate of change that is basically driven by stenosis level [29, 38]. In addition, a wavy behaviour can be usually recognized in proximity of the maximum area, EOA_{max} due to leaflets fluttering [39, 40]. Notice that this behaviour is observed also for the prosthetic valves [41 - 44].

The scenario here described is the focus of the model developed in the following section.

2.2. Analytical Model of Δp_{net}

Some assumptions are required to develop the mathematical formulation of the pressure drop experienced by blood flow between locations 1 and 2 in Fig. (**1a**). Firstly, blood is considered Newtonian and incompressible, and non-deformable walls are assumed for the tube, *i.e.*, the area A of the tube is constant not only along its axis *x* but also in time *t*. As a result, from mass conservation, the instantaneous flow rate Q(t) turns out to be the same at each tube section. Secondly, the area of the orifice is assumed to vary in time and,
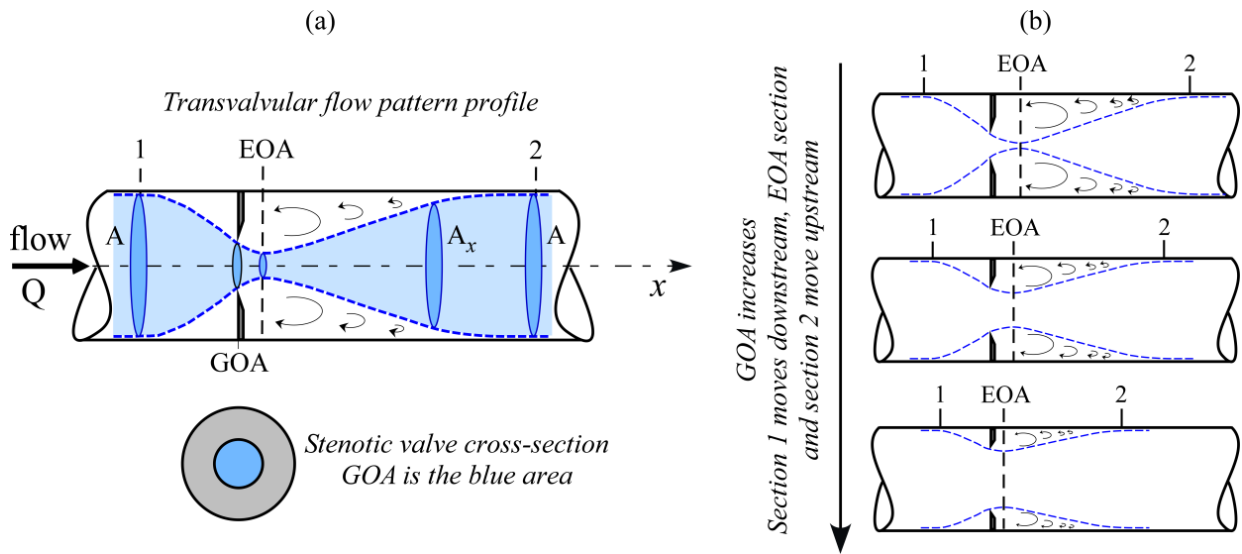
(a)

Transvalvular flow pattern profile

(b)

Fig. (1). Panel (a): schematic representation of the instantaneous flow pattern through the aortic valve. Notations are as follows: GOA: geometric orifice area, *i.e.* the area of the stenotic valve orifice; EOA: effective orifice area, *i.e.* the area of the jet at vena contracta section. Sections 1 and 2 are located in the left ventricular outflow tract and ascending aorta, respectively. Panel (b): instantaneous flow pattern as the GOA increases during the valve opening phase.

as a consequence, the whole transvalvular jet dynamics is accounted for. This latter assumption implies that, in particular, the effective orifice area and the length of the jet are time-dependent, *i.e.* EOA(t) and L(t) have to be considered.

By neglecting the weight of the fluid in the tube [19], the total head of the flow at any section, H is

$$H = \frac{p}{\gamma} + \alpha \frac{V^2}{2g} \qquad (1)$$

where g is gravity, γ is the specific weight of the fluid, p is the pressure, V is the average flow velocity (*i.e.* the ratio of the flow rate to the jet cross-sectional area), and α is a correction factor which accounts for non uniform velocity distribution across a given cross-section [45]. Notice that V, p and H are all time-dependent.

The total head at any time varies with the distance along the flow direction, *x* according to the following equation [37]

$$\frac{\partial H}{\partial x} = -\frac{1}{g}\beta \frac{\partial V}{\partial t} - J \qquad (2)$$

where J is the head loss per unit length of flow, and β is another correction factor accounting for non-uniform velocity distribution. Here, almost uniform velocity profiles are assumed at any section along the jet [19, 35], so that $\alpha \cong \beta \cong 1$.

Equation (1) shows that the instantaneous pressure difference $\Delta p_{net} = (p_1 - p_2)/\gamma$, *i.e.* the *net* pressure drop across the orifice, is equal to the instantaneous total head difference ($H_1 - H_2$) since sections 1 and 2 have the same cross-sectional area

and, hence, the same average velocity. Hence, from integration of Equation (2) between locations 1 and 2, Δp_{net} is obtained

$$\Delta p_{net} = H_1 - H_2 = \frac{1}{g}\int_1^2 \frac{\partial V}{\partial t}dx + \Delta H_{12} \qquad (3)$$

where $\Delta H_{12} = \int_1^2 Jdx$ is the head loss due to both viscous shear along the wall and boundary layer separation. For orifice flow, the latter source of loss is larger than the former one [45], and is therefore the only contribution taken into account here. Moreover, turbulent recirculation mainly affects the flow from EOA location to location 2, so that $\Delta h_{12} = \Delta h_{EOA2}$ is assumed [46].

The head loss Δh_{EOA2} can be obtained by integrating equation (2) from EOA to location 2, and is expressed as

$$\Delta H_{EOA2} = \int_{EOA}^2 Jdx = \frac{p_{EOA} - p_2}{\gamma} + $$
$$\frac{V_{EOA}^2 - V_2^2}{2g} - \frac{1}{g}\int_{EOA}^2 \frac{\partial V}{\partial t}dx \qquad (4)$$

In order to express the pressure difference $=(p_{EOA}-p_2)/\gamma$ in terms of average velocities, the momentum equation along *x* is applied to the control volume Ω shown in Fig. (**2a**)

$$p_{EOA}A + \rho Q V_{EOA} - p_2 A - \rho Q V_2 = \rho \int_\Omega \frac{\partial V}{\partial t}d\Omega \qquad (5)$$
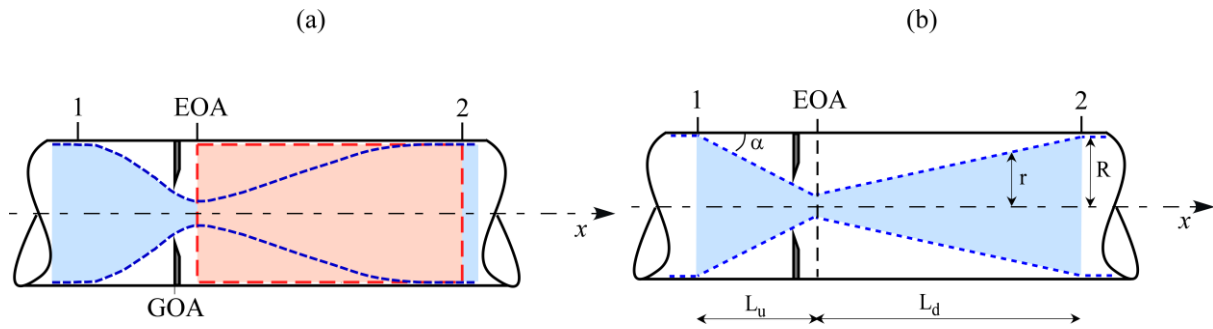
Fig. (2). Panel (a): the control volume Ω between locations EOA and 2 is shown as a light red area; panel (b): conical contracting and expanding jets adopted to model the transvalvular flow, with adopted notations.

Recalling that $d\Omega = Adx$, and $Q = AV_2$, Equation (5) gives

$$\frac{p_{EOA} - p_2}{\gamma} = \frac{V_2}{g}\left(V_2 - V_{EOA}\right) + \frac{1}{g}\int_{EOA}^{2}\frac{\partial V}{\partial t}dx \qquad (6)$$

Equations (3), (4), and (6) then give

$$\Delta p_{net} = \frac{\left(V_2 - V_{EOA}\right)^2}{2g} + \frac{1}{g}\int_{1}^{2}\frac{\partial V}{\partial t}dx \qquad (7)$$

According to mass conservation one has $Q = EOA \cdot V_{EOA} = AV_2 = A_x V$, and Equation (7) is hence rewritten as

$$\Delta p_{net} = \frac{Q^2}{2g}\left(\frac{1}{EOA} - \frac{1}{A}\right)^2 + \frac{1}{g}\int_{1}^{2}\frac{\partial}{\partial t}\left(\frac{Q}{A_x}\right)dx \qquad (8)$$

Moreover, recalling that $Q = Q(t)$ and $A_x = A_x(x,t)$, the local inertia term on the right side of Equation (8) can be splitted in two terms, so that Δp_{net} is expressed as

$$\Delta p_{net} = \frac{Q^2}{2g}\left(\frac{1}{EOA} - \frac{1}{A}\right)^2 + \frac{1}{g}\frac{\partial Q}{\partial t}\int_{1}^{2}\frac{1}{A_x}dx$$
$$- \frac{Q}{g}\int_{1}^{2}\frac{1}{A_x^2}\frac{\partial A_x}{\partial t}dx \qquad (9)$$

the three terms on the right hand side being the *head loss* term (Δ_{Loss}), the inertia term depending on flow pulsatility (*flow inertia,* Δ_{fl}), and the inertia term related to the time variability of transvalvular jet geometry (*jet inertia,* Δ_{jl}), respectively. Notice that the latter is the novel contribution proposed by the present model.

Both Δ_{fl} and Δ_{jl} require the instantaneous geometry of the jet (*i.e.* $A_x(x,t)$) to be evaluated. In order to obtain an analytical formulation for them, the contracting and the expanding jet are assumed conical (Fig. **2b**). Equation (10) can thus be

rearranged (see Appendix for details)

$$\Delta p_{net} = \frac{Q^2}{2g}\left(\frac{1}{EOA} - \frac{1}{A}\right)^2 + \frac{Q}{g}\left[\left(\frac{1}{Q}\frac{\partial Q}{\partial t} - \frac{1}{2EOA}\frac{\partial EOA}{\partial t}\right)\frac{L}{\sqrt{A \cdot EOA}} - \frac{\partial L}{\partial t}\frac{\sqrt{A/EOA} - 1}{\sqrt{A \cdot EOA}}\right] \qquad (10)$$

where L is the instantaneous total length of the jet.

Time behaviour of the total length of the jet, L is required to calculate the instantaneous net pressure difference as given by Equation (10). For conical jet configuration the following relation holds (see Appendix)

$$\int_{1}^{2}\frac{1}{A_x}dx = \frac{L}{\sqrt{A \cdot EOA}} \qquad (11)$$

Moreover, according to Garcia and colleagues [19] it turns out that

$$\int_{1}^{2}\frac{1}{A_x}dx = \frac{2\pi}{\sqrt{A}}\sqrt{\frac{A}{EOA} - 1} \qquad (12)$$

Hence, from Equations (11) and (12), the length of the jet can be expressed as

$$L = 2\pi\sqrt{A - EOA} \qquad (13)$$

so that, with Equation (13), Equation (10) finally reads

$$\Delta p_{net} = \frac{Q^2}{2g}\left(\frac{1}{EOA} - \frac{1}{A}\right)^2 + \frac{2\pi Q}{g}\left[\frac{1}{Q}\frac{\partial Q}{\partial t}\sqrt{\left(\frac{1}{EOA} - \frac{1}{A}\right)} - \frac{1}{2EOA}\frac{\partial EOA}{\partial t}\left(\frac{1}{\sqrt{EOA}} - \frac{1}{\sqrt{A}}\right)\frac{\sqrt{A/EOA}}{\sqrt{A/EOA - 1}}\right] \qquad (14)$$

Equation (14) can hence be adopted to predict the waveform of Δp_{net} for assigned values of A and temporal distribution of the ejected Q(t) once EOA(t) is known.
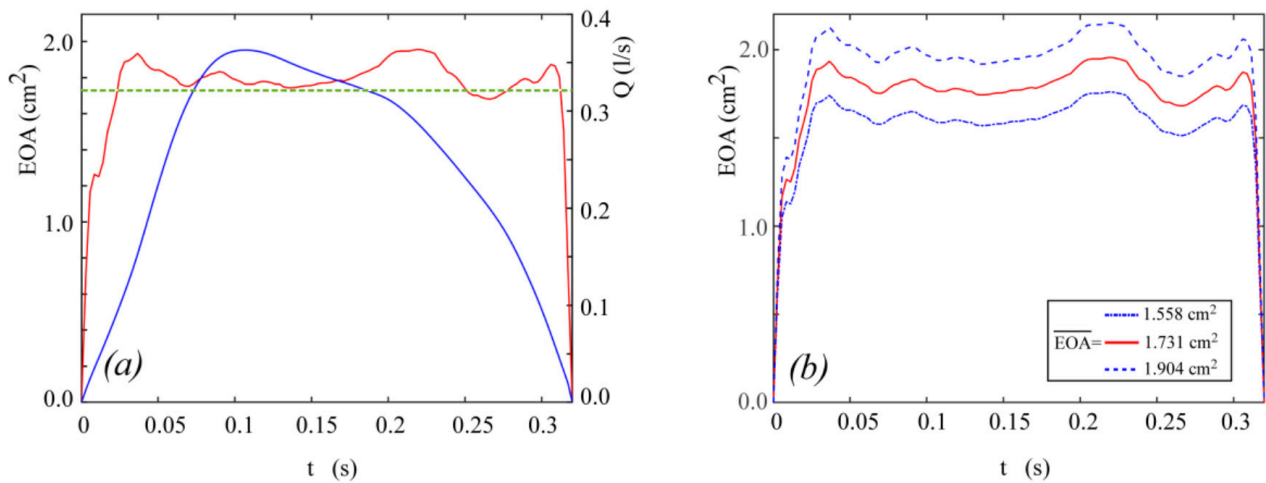
Fig. (3). Panel a: the *in-vitro* flow rate (blue line, taken from Fig. 4 of [19]) and effective orifice area (red line, taken from [29]) waveforms adopted for the complete unsteady Δp_{net} model validation. The green dotted line corresponds to the mean effective orifice area according to [19]. Panel (b): EOA(t) waveforms adopted for the sensitivity analysis as $\overline{EOA}$ varies.
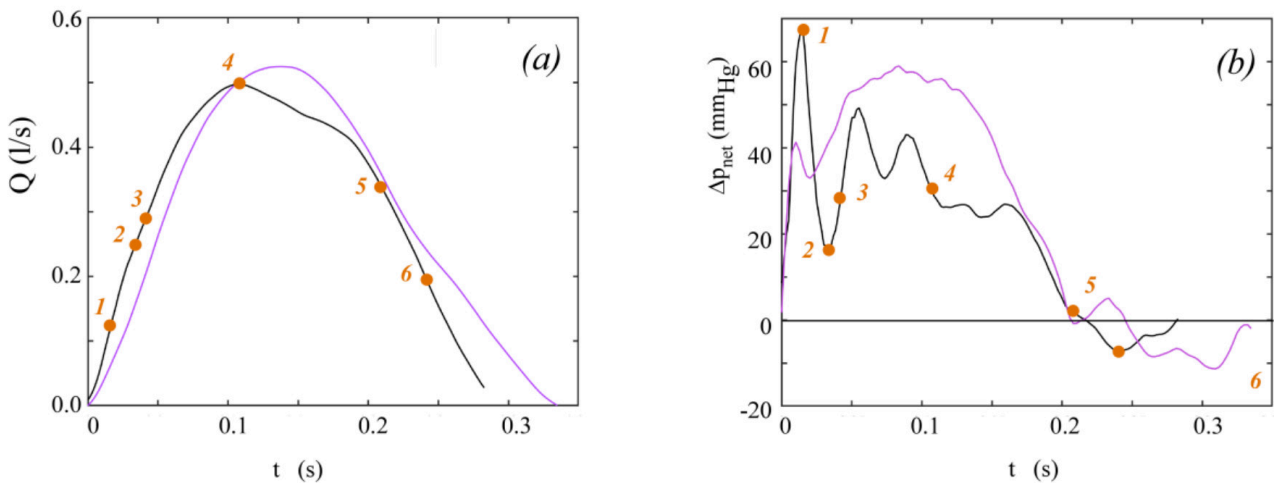

Fig. (4). *in-vitro* flow rate (panel a) and net pressure drop (panel b) used as input for Equation (15) solution. Black lines show data taken from [23], purple lines show data taken from [19]. Orange dots mark significant time points (see also Fig. (**6**)).

2.3. The Model of ΔP_{net} as a Numerical Tool for EOA(t) Calculation

Equation (14) can be rearranged to obtain the rate of change of the effective orifice area

$$\frac{\partial EOA}{\partial t} = \left\{ \left[\frac{1}{Q} \frac{\partial Q}{\partial t} \sqrt{\left(\frac{1}{EOA} - \frac{1}{A}\right)} + \left[\frac{Q^2}{2g} \left(\frac{1}{EOA} - \frac{1}{A}\right)^2 - \Delta p_{net} \right] \frac{g}{2\pi Q} \right\} \cdot$$
$$\cdot 2EOA \left(\frac{1}{\sqrt{EOA}} - \frac{1}{\sqrt{A}} \right)^{-1} \frac{\sqrt{A/EOA - 1}}{\sqrt{A/EOA}} \qquad (15)$$

Equation (15) is a nonlinear partial differential equation of the first order in EOA that can be solved numerically for given temporal distributions of $\Delta p_{net}(t)$ and Q(t). Here a 4ᵗʰ order Runge-Kutta scheme is adopted, for prescribed initial condition EOA(t)=EOA.

2.4. Numerical Tests

Data from published *in-vitro* tests [19] are here used to validate Equation (14). In particular, the waveforms of p_1, p_2, and Q drawn in Fig. (**4**) of [19] are digitized in the ejection period T_{ej} to obtain the numerical values of these quantities. The instantaneous derivative $\partial Q/\partial t$ required in Equation (14) is approximated by central differences. In addition, an aortic area A=800 mm² and a fluid density ρ=1008 kg/m³ are assumed, as in the experimental test [19]. Unfortunately, the temporal distribution of the effective orifice area is not given in [19]. A realistic behaviour is hence here reconstructed as follows. The non-dimensional effective orifice area EOA$_{nd}$(t)=EOA(t)/EOA$_{max}$ given in [29] for aortic healthy valve is assumed, with open valve duration T_{op} equal to T_e. Moreover, the maximum area EOA$_{max}$ is estimated as
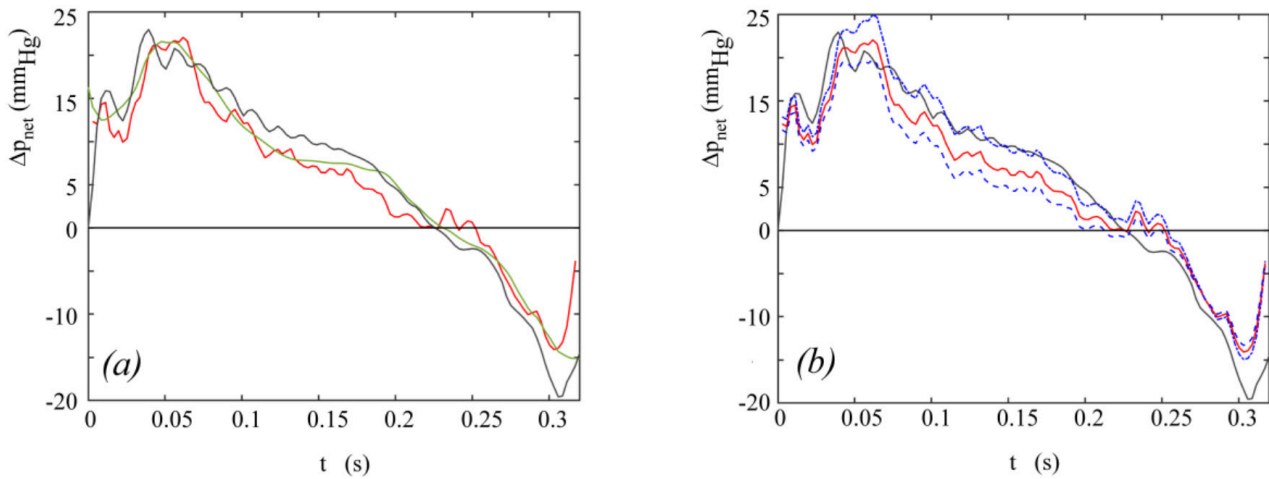
Fig. (5). Net pressure drop model validation and sensitivity analysis results. Panel a: *in-vitro* (grey line) and predicted net pressure drop (red line: present Δp_{net} model; green line: model given in [19]. $\overline{EOA}$ = 1.731 cm^2 for both models). Panel b: grey and red lines as in panel a; blue lines: Δp_{net} as predicted by the present model for $\overline{EOA}$ = 1.558 cm^2 (upper line) and $\overline{EOA}$ = 1.904 cm^2 (lower line), respectively *in-vitro* data are taken from [19].
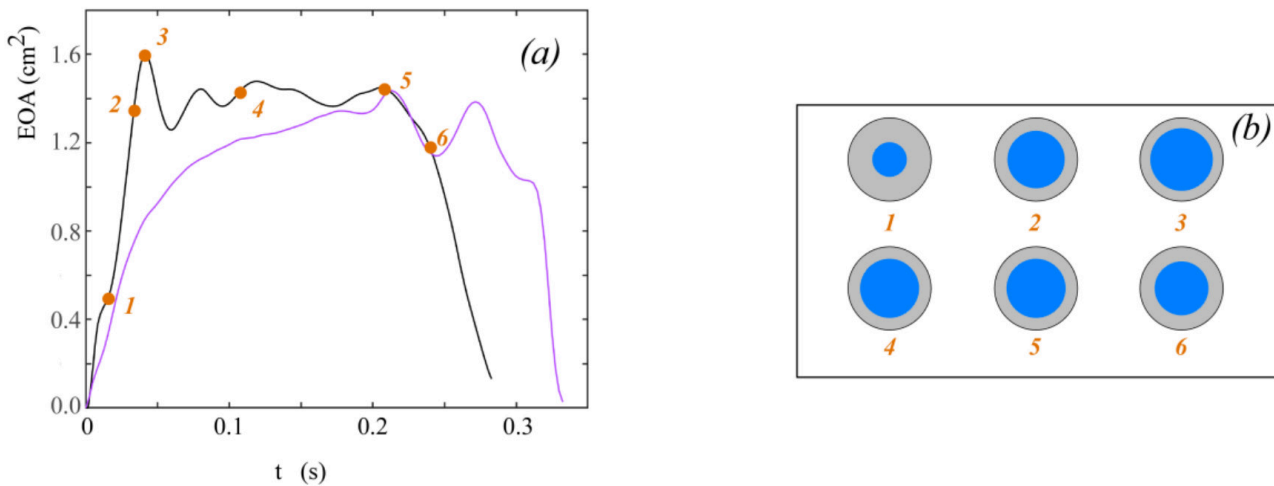

Fig. (6). Instantaneous effective orifice area calculated by solving Equation (15) (colours as in Fig. 4). Panel (d): schematic representation of calculated EOA(t) at significant time points for data taken from [23]. Orange dots mark significant time points (see also Fig. (**4**).

$$EOA_{max} = \frac{\overline{EOA}}{EOA_{nd}} \qquad (16)$$

where the overbar denotes the mean over the ejection period. Finally, the mean area $\overline{EOA}$ is calculated by adopting the formula reported by Garcia and colleagues [19]

$$\overline{EOA} = \frac{1}{A} + \sqrt{2g\frac{\overline{\Delta p_{net}}}{\overline{Q^2}}} \qquad (17)$$

For the *in-vitro* conditions taken from [19] and here considered, $\overline{EOA}$ = 1.731 cm^2. The behaviour of Q(t) and EOA(t) obtained in the above way and implemented in Equation (14) is shown in Fig. (**3a**).

It is worthwhile underlining that Equation (17) was obtained in [19] under the hypothesis that the valve dynamics keeps constant in time. As a consequence, the mean effective orifice here calculated is somehow different from the actual one. For that reason, the sensitiveness of Δp_{net} to the value assigned to $\overline{EOA}$ is here investigated by implementing Equation (14) for $\overline{EOA} = (1.731 \pm 0.1 \cdot 1.731)$ cm^2, while maintaining EOA$_{nd}$(t) and Q(t) unchanged. Notice that as $\overline{EOA}$ varies the rate of change $\partial EOA/\partial t$ proportionally varies (*i.e.* larger/smaller $\overline{EOA}$ implies faster/slower EOA variation in time). Fig. (**3b**) shows the different waveforms of EOA(t) here adopted for the sensitivity analysis.

Further tests are here performed to explore the capability of the model of Δp_{net} to serve as a numerical tool for EOA(t)

calculation. In this series of tests, $Q(t)$ and $\Delta p_{net}(t)$ waveforms measured in two different literature *in-vitro* experiments are used as input of the numerical scheme adopted to solve Equation (15). The considered data are shown in Figs. (**4a**) and (**4b**). They have been measured for a bileaflet mechanichal valve (Saint Jude Hp 19 mm, [23]), and for a biological valve (Mosaic 21 mm, [19]), respectively. Notice that since the flow rate corresponding to the Mosaic 21 mm valve experiment has not been reported in [19], it is here calculated according to the following approach. First, the analytical model of the net pressure gradient proposed in [19] is rewritten in the form:

$$\frac{\partial Q}{\partial t} = \frac{g}{2\pi} \frac{1}{\sqrt{\left(\frac{1}{\overline{EOA}} - \frac{1}{A}\right)}} \left[\Delta p_{net} - \frac{Q^2}{2g}\left(\frac{1}{\overline{EOA}} - \frac{1}{A}\right)^2 \right] \quad \textbf{(18)}$$

Second, the instantaneous net pressure drop for the Mosaic 21 mm valve predicted by Garcia and co-authors is digitized from Fig. (**6**) of [19]; notice that the corresponding $\overline{EOA}$ is also reported in the that figure, and the ventricular-aortic area A is reported in the text. Finally, Equation (18) is solved for the aforesaid values of Δp_{net}, $\overline{EOA}$ and A, so that the instantaneous experimental $Q(t)$ is obtained. In both the present numerical tests, integration of Equation (15) starts from an instant t immediately after the beginning of ejection (*i.e.*, immediately after the valve starts to open) so that the initial value $EOA(t)=\overline{EOA}$ is small but not null.

3. RESULTS

The instantaneous net pressure drop predicted by the present model for the hemodynamic conditions depicted in Fig. (**3a**) is shown in Fig. (**5a**), together with the Δp_{net} waveform measured in *in-vitro* tests [19]. The instantaneous net pressure drop predicted by the model given in [19] for an effective orifice area constant in time and equal to $\overline{EOA} = 1.731$ cm^2 is also shown for comparison.

The results of the sensitivity analysis of Equation (14) performed by varying the mean effective orifice area $\overline{EOA}$ are reported in Fig. (**5b**).

Fig. (**6a**) shows the instantaneous effective orifice area in time as calculated from Equation (15) for the experiments reported in the two studies [23] and [19], respectively. For the experiment reported by Fiore *et al.* [23], the schematic representation of the effective orifice area cross-section at significant time points is also given for a comprehensive view of the phenomenon (Fig. **6b**).

4. DISCUSSION

The *complete unsteady* Δp_{net} model here proposed can be regarded as an upgrade of that developed earlier [19]. Basically, the hypotheses adopted to describe the flow across an aortic valve are the same but, as novel contribution of the present work, the effects of valve dynamics are accounted for. Moreover, the transvalvular flow pattern is here modelled as a conical jet, which allows the analytical integration of the inertia term and leads to Equation (10), with $\Delta p_{net}(t)$ expressed as a

function of $Q(t)$, $EOA(t)$ and $L(t)$. In particular, it is found that: i) transvalvular jet inertia contributes to Δp_{net} through the rate of change of both the effective orifice area, EOA and the length of the jet, L; ii) time-variability of EOA affects not only the novel jet inertia term Δ_{jl} but also the flow inertia term Δ_{fl} and the head loss term Δ_{Loss}, since they both depend on $EOA(t)$; iii) for rigid orifices (*i.e.* $\partial EOA/\partial t \to 0$ and $\partial L/\partial t \to 0$) Equation (10) reduces to the model developed by Garcia and colleagues [19] following a semi-empirical approach, thus corroborating the present choice of a conical shape for the converging/ diverging transvalvular jet.

A simpler formulation of the model is also given (Equation (14)), which can be easily implemented once purely kinematic and geometrical quantities ($Q(t)$, $EOA(t)$, and A) are known. Notice that the required data can be obtained by routine Doppler echocardiography for both the *in-vitro* and *in-vivo* case, *i.e.* the model allows non-invasive estimation of Δp_{net}. Equation (14) is validated by comparing its prediction to published experimental data and to the results provided by the model given in [19] (Fig. **5a**). The ability of the present model to capture Δp_{net} oscillations occurring at early/late ejection as the valve rapidly opens/closes clearly appears from the comparison. Moreover, the wavy Δp_{net} behaviour due to valve leaflets fluttering in the open valve phase is well reproduced. Hence, both these features actually result to be the footprints of the valvular dynamics, since they are reproduced only when valve dynamics effects are accounted for. It is worthwhile now recalling that the behaviour of $EOA(t)$ adopted in Equation (14) validation is not the real one but a realistic reconstruction, built from *in-vivo* measurements of healthy aortic valve dynamics. The mean effective orifice area, which is also required to reconstruct $EOA(t)$, is estimated from the theory reported in [19], *i.e.* under the hypothesis of valve dynamics constant in time. The results of the sensitivity analysis performed on Equation (14) for values of $\overline{EOA}$ around such an estimate show that the correspondence between the predicted and the *in-vitro* Δp_{net} can even improve if an appropriate $\overline{EOA}$ is adopted (Fig. **5b**). That is, a very good match between the calculated and the experimental net pressure drop is likely to result when the real rather than the reconstructed $EOA(t)$ is available. However, it is worthwhile pointing out that the difference between the net pressure drop predicted by Equation (14) for $\overline{EOA} = 1.731$ cm^2 and the experimental one shown in Fig. (**5a**) results to be less than 5 mmHg (*i.e.* in the range of clinical accuracy) in the entire ejection period, apart from the late systole, when valve closure occurs and the difference reaches a maximum of about 10 mm$_{hg}$. This latter result, which is however limited to a narrow time span, suggests that the predicted Δp_{net} is likely quite sensitive to the actual $EOA(t)$ in the final valve closing phase. All the above results strengthen the idea that aortic valve dynamics plays a non-negligible role on the time evolution of net pressure drop across the valve. Despite the overall complexity of the flow field, such a contribution seems to be accurately predicted by the simple one-dimensional approach here proposed. Interestingly, the analytical expression of the jet inertia term Δ_{jl} in Equation (14) shows that it has a sign opposite to that of the flow inertia term Δ_{fl}, so that a reduction of Δp_{net} is favoured while the flow rate

increases.

The present theoretical framework on transaortic hemodynamics also provides a partial differential equation for the effective orifice area rate of change. This tool can be adopted to calculate EOA(t) once the flow rate and net pressure drop are known. Numerical solution of this equation for two literature cases (Fig. **5a**) indicates that all the fundamental phases and features that typically mark aortic valve/jet dynamics (opening, maximum opening and concurrent fluttering, closing) are effectively reproduced. Indeed, EOA (t) exhibits a behaviour remarkably similar to what obtained in *in-vivo*, *in-vitro* and (sophisticated) *in-silico* investigations for either the geometrical, the projected, and the effective orifice area [25, 38, 40, 47, 48]. Notice that although these areas pertain to different cross sections along the downstream jet and their values may hence noticeably differ for the same valve [41, 49], they all show similar evolution in time, that can be compared. Finally, it is worthwhile observing that the above results also constitute an indirect (but robust) validation of the Δp_{net} analytical model.

4.1. Study Limitations

The ejection period rather than the entire systole is considered in the theoretical model of Δp_{net}. The model thus applies to positive flow rate (forward flow) only. However, the brief backward flow ($Q(t)<0$) that usually occurs in the late systole can be accounted for by substituting $Q|Q|$ to Q^2.

The ejection period, T_{ej} and the open valve phase duration, T_{op} are assumed equal when solving Equation (14), for the sake of simplicity. Notice that attributing a specific value to T_{op} would be somehow arbitrary. However, additional calculations performed with $T_{op}=(1.05-1.2)T_{ej}$ show that the correspondence of predicted *in-vitro* Δp_{net} can even improve with respect to the result shown in Fig. (**5a**).

Some assumptions (*i.e.*, flat velocity profiles in the core of the transvalvular jet, length jet as a function of aortic area only rather than of the Reynolds number too) indirectly imply turbulent flow conditions. However, since transvalvular flow is typically recognized as transient [49] the adopted assumptions seems acceptable.

4.2. Future Developments

Ad-hoc *in-vitro* tests for comprehensive validation of both the Δp_{net} model and the EOA(t) computational tool are in progress. The quantities that are going to be monitored are $Q(t)$, $p_1(t)$ and $p_2(t)$, and $V_1(t)$. The latter is necessary to estimate the experimental instantaneous effective orifice area as $Q/(A.V_1)$. High-speed video of the geometrical/projected orifice area will also be recorded, to compare time evolution of geometrical/projected/effective orifice area. Both bioprostheses and mechanical valves are planned to be tested, in order to analyse the ability of the model to describe transvalvular hemodynamics through 'funnel type' and non-circular, non-single orifices. Prostheses will also be artificially stenotized to examine main hemodynamic parameters (both predicted and experimental) as valve stenosis grade varies, when important valve dynamics effects are expected.

In-vivo application of the present theoretical approach is also planned, with two main aims: i) compare model and catheterization Δp_{net}; ii) deeply analyse the relationship between the tranvalvular drop routinely estimated by echocardiography to grade aortic stenosis and that predicted by the complete unsteady model. Both the above points are intended for a cohort of patients as large and various as possible. The idea is that provided point i) will give reliable results, point ii) will help in understanding sources and magnitudes of inconsistencies between guidelines and diagnostics, thus contributing to the improvement of aortic stenosis assessment.

CONCLUSION

Accurate and unique assessment of aortic stenosis by non-invasive quantification of hemodynamic parameters that consistently reflect ventricular overload is an open question yet. The net transvalvular pressure drop has been recognized as one of the markers that might help in closing the debate. The present analytical formulation of $\Delta p_{net}(t)$ is proposed as a simple but complete tool that may be easily adopted in the clinical practice. The model requires only a limited number of data that can be acquired by routine echo-Doppler, and accounts not only for pressure loss and flow inertia contributions but also for transvalvular jet inertia effects due to valve leaflets movement. Model prediction is compared to *in-vitro* data and a satisfactory correspondence is found. In particular, the model turns out to reliably capture pressure drop oscillations due to valve dynamics. The present theoretical approach also provides a novel tool for the estimation of the instantaneous effective orifice area, which may be used in either *in-vitro* laboratories or catheterization rooms as an alternative to continuity equation.

ETHICS APPROVAL AND CONSENT TO PARTI-CIPATE

Not applicable.

HUMAN AND ANIMAL RIGHTS

No animals/humans were used for studies that are the basis of this research.

CONSENT FOR PUBLICATION

Not applicable.

AVAILABILITY OF DATA AND MATERIALS

Not applicable.

FUNDING

The study was funded by the University of Padova PRAT grant (Code No: CPDA130215).

CONFLICT OF INTEREST

The author declares no conflict of interest, financial or otherwise.

ACKNOWLEDGEMENTS

The work was developed under the frame of the Infrastructure of Research of the University of Padova INCAS. The author acknowledges colleagues that participated in discussing the present research.

APPENDIX

The two integrals in equation (9) are evaluated as follows.

The first integral can be expressed as

$$\int_1^2 \frac{1}{A_x} dx = \int_1^2 \frac{1}{\pi r^2} dx = \int_1^{EOA} \frac{1}{\pi r^2} dx + \int_{EOA}^2 \frac{1}{\pi r^2} dx \quad \textbf{(1)}$$

where r=r(x,t) is the radius of the jet at location x and time t.

With notations as adopted in Fig. (**1**), the integral from location 1 to location EOA can be easily evaluated and expressed as

$$\int_1^{EOA} \frac{1}{\pi r^2} dx = \int_R^{r_{EOA}} \frac{1}{\pi r^2} \frac{-dr}{\tan\alpha} = \frac{1}{\pi \tan\alpha}\left(\frac{1}{r_{EOA}} - \frac{1}{R}\right) \quad \textbf{(2)}$$

where R and r_{EOA} are the radius of the jet at locations 1 and EOA, respectively (*i.e.* at the LV outflow tract and at the vena contracta). The angle α is such that , where L_u is the length of the jet between locations 1 and EOA. Hence, equation (A2) can be rearranged as

$$\int_1^{EOA} \frac{1}{\pi r^2} dx = \frac{L_u}{\pi R r_{EOA}} \quad \textbf{(3)}$$

The same approach applied to the integral from location EOA to location 2 in equation (A1) yields

$$\int_{EOA}^2 \frac{1}{\pi r^2} dx = \frac{L_d}{\pi R r_{EOA}} \quad \textbf{(4)}$$

where L_d is the length of the jet between locations EOA and 2.

Hence, the first integral in equation (9) is simply expressed as

$$\int_1^2 \frac{1}{A_x} dx = \frac{L}{\pi R r_{EOA}} \quad \textbf{(5)}$$

where $L = L_u + L_d$ is the total length of the jet.

The second integral in equation (9) can be written as

$$\int_1^2 \frac{1}{A_x^2} \frac{\partial A_x}{\partial t} dx = \int_1^2 \frac{2}{\pi r^3} \frac{\partial r}{\partial t} dx = \int_1^{EOA} \frac{2}{\pi r^3} \frac{\partial r}{\partial t} dx + \int_{EOA}^2 \frac{2}{\pi r^3} \frac{\partial r}{\partial t} dx \quad \textbf{(6)}$$

The radius r of the jet between locations 1 and EOA is

$$r = R - x\tan\alpha \quad \textbf{(7)}$$

so that the following relations hold

$$x = \frac{R - r}{\tan\alpha}$$
$$\frac{\partial r}{\partial t} = -x \frac{\partial \tan\alpha}{\partial t} \quad \textbf{(8)}$$

Time variation of the length of the contracting jet, L_u is accounted for. Hence, the time derivative of the radius r is

$$\frac{\partial r}{\partial t} = x\left(\frac{1}{L_u} \frac{\partial r_2}{\partial t} + \frac{R - r_{EOA}}{L_u^2} \frac{\partial L_u}{\partial t} \right) \quad \textbf{(9)}$$

With equations (A8) and (A9), the integral from locations 1 to EOA in equation (A6) can be written as

$$\int_1^{EOA} \frac{2}{\pi r^3} \frac{\partial r}{\partial t} dx = \int_R^{r_{EOA}} -\frac{2L_u^2}{\pi(R - r_{EOA})^2}\left(\frac{1}{L_u}\frac{\partial r_{EOA}}{\partial t} + \frac{R - r_{EOA}}{L_u^2}\frac{\partial L_u}{\partial t} \right)\frac{(R - r)}{r^3} dr \quad \textbf{(10)}$$
$$= \frac{1}{\pi R r_{EOA}^2}\left[L_u \frac{\partial r_{EOA}}{\partial t} + (R - r_{EOA})\frac{\partial L_u}{\partial t} \right]$$

A similar approach applied to the integral extended from EOA location to location 2 in equation (A6) yields

$$\int_{EOA}^2 \frac{2}{\pi r^3} \frac{\partial r}{\partial t} dx = \frac{1}{\pi R r_{EOA}^2}\left[L_d \frac{\partial r_{EOA}}{\partial t} + (R - r_{EOA})\frac{\partial L_d}{\partial t} \right] \quad \textbf{(11)}$$

Hence, the second integral in equation (9) reads

$$\int_1^2 \frac{1}{A_x^2} \frac{\partial A_x}{\partial t} dx = \frac{1}{\pi R r_{EOA}^2}\left[L \frac{\partial r_{EOA}}{\partial t} + (R - r_{EOA})\frac{\partial L}{\partial t} \right] \quad \textbf{(12)}$$

Finally, with equations (A5) and (A12) and using the cross-sectional area instead of the radius, the local inertia term in equation (9) can be written as

$$\frac{1}{g}\left(\frac{\partial Q}{\partial t} \int_1^2 \frac{1}{A_x} dx - Q \int_1^2 \frac{1}{A_x^2} \frac{\partial A_x}{\partial t} dx \right) =$$
$$= \frac{Q}{g}\left[\left(\frac{1}{Q}\frac{\partial Q}{\partial t} - \frac{1}{2EOA}\frac{\partial EOA}{\partial t} \right)\frac{L}{\sqrt{A \cdot EOA}} - \frac{\partial L}{\partial t}\frac{\sqrt{A/EOA} - 1}{\sqrt{A \cdot EOA}} \right] \quad \textbf{(13)}$$

REFERENCES

[1]   F.M. Susin, V. Tarzia, T. Bottio, V. Pengo, A. Bagno, and G. Gerosa, "In-vitro detection of thrombotic formation on bileaflet mechanical heart valves", *J. Heart Valve Dis.,* vol. 20, no. 4, pp. 378-386, 2011. [PMID: 21863649]

[2]   C. Romata, F.M. Susin, A. Cambi, V. Tarzia, V. Pengo, G. Gerosa, and A. Bagno, "Comparative classification of thrombotic formations on bileaflet mechanical heart valves by phonographic analysis", *J. Artif. Organs,* vol. 14, no. 2, pp. 100-111, 2011. [http://dx.doi.org/10.1007/s10047-011-0562-z] [PMID: 21448607]

[3]   P. Pibarot, and J.G. Dumesnil, "Improving assessment of aortic stenosis", *J. Am. Coll. Cardiol.,* vol. 60, no. 3, pp. 169-180, 2012. [http://dx.doi.org/10.1016/j.jacc.2011.11.078] [PMID: 22789881]

[4]   A.E. Abbas, L.M. Franey, J. Goldstein, and S. Lester, "Aortic valve stenosis: to the gradient and beyond--the mismatch between area and gradient severity", *J. Interv. Cardiol.,* vol. 26, no. 2, pp. 183-194, 2013. [http://dx.doi.org/10.1111/joic.12004] [PMID: 23278313]

[5]   N. Saikrishnan, G. Kumar, F.J. Sawaya, S. Lerakis, and A.P. Yoganathan, "Accurate assessment of aortic stenosis: a review of diagnostic modalities and hemodynamics", *Circulation,* vol. 129, no. 2, pp. 244-253, 2014. [http://dx.doi.org/10.1161/CIRCULATIONAHA.113.002310] [PMID: 24421359]

[6]   G. Burriesci, P. Peruzzo, F.M. Susin, G. Tarantini, and A. Colli, "In

vitro hemodynamic testing of Amplatzer plugs for paravalvular leak occlusion after transcatheter aortic valve implantation", *Int. J. Cardiol.,* vol. 203, pp. 1093-1099, 2016.
[http://dx.doi.org/10.1016/j.ijcard.2015.11.106] [PMID: 26642371]

[7]   R. Toninato, J. Salmon, F.M. Susin, A. Ducci, and G. Burriesci, "Physiological vortices in the sinuses of Valsalva: An *in vitro* approach for bio-prosthetic valves", *J. Biomech.,* vol. 49, no. 13, pp. 2635-2643, 2016.
[http://dx.doi.org/10.1016/j.jbiomech.2016.05.027] [PMID: 27282961]

[8]   A. Colli, L. Besola, E. Bizzotto, P. Peruzzo, D. Pittarello, and G. Gerosa, "Edge-to-edge mitral valve repair with transapical neochord implantation", *J. Thorac. Cardiovasc. Surg.,* vol. 156, no. 1, pp. 144-148, 2018.
[http://dx.doi.org/10.1016/j.jtcvs.2018.02.008] [PMID: 29510937]

[9]   B. Rahmani, S. Tzamtzis, H. Ghanbari, G. Burriesci, and A.M. Seifalian, "Manufacturing and hydrodynamic assessment of a novel aortic valve made of a new nanocomposite polymer", *J. Biomech.,* vol. 45, no. 7, pp. 1205-1211, 2012.
[http://dx.doi.org/10.1016/j.jbiomech.2012.01.046] [PMID: 22336198]

[10]   A. Kheradvar, E.M. Groves, A. Falahatpisheh, M.K. Mofrad, S. Hamed Alavi, R. Tranquillo, L.P. Dasi, C.A. Simmons, K. Jane Grande-Allen, C.J. Goergen, F. Baaijens, S.H. Little, S. Canic, and B. Griffith, "Emerging trends in heart valve engineering: part IV. Computational modeling and experimental studies", *Ann. Biomed. Eng.,* vol. 43, no. 10, pp. 2314-2333, 2015.
[http://dx.doi.org/10.1007/s10439-015-1394-4] [PMID: 26224522]

[11]   V. Raghav, I. Okafor, M. Quach, L. Dang, S. Marquez, and A.P. Yoganathan, "Long-term durability of Carpentier-Edwards Magna Ease valve: A one billion cycle *in vitro* study", *Ann. Thorac. Surg.,* vol. 101, no. 5, pp. 1759-1765, 2016.
[http://dx.doi.org/10.1016/j.athoracsur.2015.10.069] [PMID: 2680 6168]

[12]   K. Vahidkhah, D. Cordasco, M. Abbasi, L. Ge, E. Tseng, P. Bagchi, and A.N. Azadani, "Flow-induced damage to blood cells in aortic valve stenosis", *Ann. Biomed. Eng.,* vol. 44, no. 9, pp. 2724-2736, 2016.
[http://dx.doi.org/10.1007/s10439-016-1577-7] [PMID: 27048168]

[13]   R. Toninato, G. Fadda, and F.M. Susin, "A red blood cell model to estimate the hemolysis fingerprint of cardiovascular devices", *Artif. Organs,* vol. 42, no. 1, pp. 58-67, 2018.
[http://dx.doi.org/10.1111/aor.12937] [PMID: 28722138]

[14]   J.I.E. Hoffman, and S. Kaplan, "The incidence of congenital heart disease", *J. Am. Coll. Cardiol.,* vol. 39, no. 12, pp. 1890-1900, 2002.
[http://dx.doi.org/10.1016/S0735-1097(02)01886-7] [PMID: 1208 4585]

[15]   T.A. Pawade, D.E. Newby, and M.R. Dweck, "Calcification in aortic stenosis: The skeleton key", *J. Am. Coll. Cardiol.,* vol. 66, no. 5, pp. 561-577, 2015.
[http://dx.doi.org/10.1016/j.jacc.2015.05.066] [PMID: 26227196]

[16]   R.O. Bonow, B.A. Carabello, K. Chatterjee, A.C. de Leon Jr, D.P. Faxon, M.D. Freed, W.H. Gaasch, B.W. Lytle, R.A. Nishimura, P.T. O'Gara, R.A. O'Rourke, C.M. Otto, P.M. Shah, J.S. Shanewise, S.C. Smith Jr, A.K. Jacobs, C.D. Adams, J.L. Anderson, E.M. Antman, V. Fuster, J.L. Halperin, L.F. Hiratzka, S.A. Hunt, B.W. Lytle, R. Nishimura, R.L. Page, and B. Riegel, "ACC/AHA 2006 guidelines for the management of patients with valvular heart disease: A report of the American College of Cardiology/American Heart Association Task Force on Practice Guidelines (writing Committee to Revise the 1998 guidelines for the management of patients with valvular heart disease) developed in collaboration with the Society of Cardiovascular Anesthesiologists endorsed by the Society for Cardiovascular Angiography and Interventions and the Society of Thoracic Surgeons", *J. Am. Coll. Cardiol.,* vol. 48, no. 3, pp. e1-e148, 2006.
[http://dx.doi.org/10.1016/j.jacc.2006.05.021] [PMID: 16875962]

[17]   A. Kanwar, J.J. Thaden, and V.T. Nkomo, "Management of patients with aortic valve stenosis", *Mayo Clin. Proc.,* vol. 93, no. 4, pp. 488-508, 2018.
[http://dx.doi.org/10.1016/j.mayocp.2018.01.020] [PMID: 29622096]

[18]   K.K. Stout, and C.M. Otto, "Quantification of valvular aortic stenosis", *ACC Curr. J. Rev.,* vol. 12, no. 2, pp. 54-58, 2003.
[http://dx.doi.org/10.1016/S1062-1458(03)00104-1]

[19]   D. Garcia, P. Pibarot, and L-G. Durand, "Analytical modeling of the instantaneous pressure gradient across the aortic valve", *J. Biomech.,* vol. 38, no. 6, pp. 1303-1311, 2005.
[http://dx.doi.org/10.1016/j.jbiomech.2004.06.018] [PMID: 15863115]

[20]   C.W. Akins, B. Travis, and A.P. Yoganathan, "Energy loss for evaluating heart valve performance", *J. Thorac. Cardiovasc. Surg.,*

vol. 136, no. 4, pp. 820-833, 2008.
[http://dx.doi.org/10.1016/j.jtcvs.2007.12.059] [PMID: 18954618]

[21]   D. Garcia, J.G. Dumesnil, L-G. Durand, L. Kadem, and P. Pibarot, "Discrepancies between catheter and Doppler estimates of valve effective orifice area can be predicted from the pressure recovery phenomenon: practical implications with regard to quantification of aortic stenosis severity", *J. Am. Coll. Cardiol.,* vol. 41, no. 3, pp. 435-442, 2003.
[http://dx.doi.org/10.1016/S0735-1097(02)02764-X] [PMID: 1257 5972]

[22]   J. Bermejo, J.C. Antoranz, I.G. Burwash, J.L. Alvarez, M. Moreno, M.A. García-Fernández, and C.M. Otto, "in-vivo analysis of the instantaneous transvalvular pressure difference-flow relationship in aortic valve stenosis: Implications of unsteady fluid-dynamics for the clinical assessment of disease severity", *J. Heart Valve Dis.,* vol. 11, no. 4, pp. 557-566, 2002.
[PMID: 12150306]

[23]   G.B. Fiore, M. Grigioni, C. Daniele, G. D'Avenio, V. Barbaro, and R. Fumero, "Hydraulic functional characterisation of aortic mechanical heart valve prostheses through lumped-parameter modelling", *J. Biomech.,* vol. 35, no. 10, pp. 1427-1432, 2002.
[http://dx.doi.org/10.1016/S0021-9290(02)00177-X] [PMID: 1223 1289]

[24]   Z. Keshavarz-Motamed, P.K. Motamed, and N. Maftoon, "Non-invasive determination of transcatheter pressure gradient in stenotic aortic valves: an analytical model", *Med. Eng. Phys.,* vol. 37, no. 3, pp. 321-327, 2015.
[http://dx.doi.org/10.1016/j.medengphy.2015.01.003] [PMID: 2568 2932]

[25]   Y. Aboelkassem, D. Savic, and S.G. Campbell, "Mathematical modeling of aortic valve dynamics during systole", *J. Theor. Biol.,* vol. 365, pp. 280-288, 2015.
[http://dx.doi.org/10.1016/j.jtbi.2014.10.027] [PMID: 25451522]

[26]   M. Arsenault, N. Masani, G. Magni, J. Yao, L. Deras, and N. Pandian, "Variation of anatomic valve area during ejection in patients with valvular aortic stenosis evaluated by two-dimensional echocardiographic planimetry: comparison with traditional Doppler data", *J. Am. Coll. Cardiol.,* vol. 32, no. 7, pp. 1931-1937, 1998.
[http://dx.doi.org/10.1016/S0735-1097(98)00460-4] [PMID: 9857874]

[27]   J. Bermejo, J.C. Antoranz, M.A. García-Fernández, M.M. Moreno, and J.L. Delcán, "Flow dynamics of stenotic aortic valves assessed by signal processing of Doppler spectrograms", *Am. J. Cardiol.,* vol. 85, no. 5, pp. 611-617, 2000.
[http://dx.doi.org/10.1016/S0002-9149(99)00820-6] [PMID: 1107 8276]

[28]   R. Shandas, J. Kwon, and L. Valdes-Cruz, "A method for determining the reference effective flow areas for mechanical heart valve prostheses: in vitro validation studies", *Circulation,* vol. 101, no. 16, pp. 1953-1959, 2000.
[http://dx.doi.org/10.1161/01.CIR.101.16.1953] [PMID: 10779462]

[29]   L.M. Beauchesne, R. deKemp, K.L. Chan, and I.G. Burwash, "Temporal variations in effective orifice area during ejection in patients with valvular aortic stenosis", *J. Am. Soc. Echocardiogr.,* vol. 16, no. 9, pp. 958-964, 2003.
[http://dx.doi.org/10.1016/S0894-7317(03)00472-3] [PMID: 1293 1108]

[30]   M. Handke, G. Heinrichs, F. Beyersdorf, M. Olschewski, C. Bode, and A. Geibel, "*In vivo* analysis of aortic valve dynamics by transesophageal 3-dimensional echocardiography with high temporal resolution", *J. Thorac. Cardiovasc. Surg.,* vol. 125, no. 6, pp. 1412-1419, 2003.
[http://dx.doi.org/10.1016/S0022-5223(02)73604-0] [PMID: 12830 062]

[31]   P.N. Watton, X.Y. Luo, X. Wang, G.M. Bernacca, P. Molloy, and D.J. Wheatley, "Dynamic modelling of prosthetic chorded mitral valves using the immersed boundary method", *J. Biomech.,* vol. 40, no. 3, pp. 613-626, 2007.
[http://dx.doi.org/10.1016/j.jbiomech.2006.01.025] [PMID: 16584739]

[32]   R. Halevi, A. Hamdan, G. Marom, K. Lavon, S. Ben-Zekry, E. Raanani, D. Bluestein, and R. Haj-Ali, "Fluid-structure interaction modeling of calcific aortic valve disease using patient-specific three-dimensional calcification scans", *Med. Biol. Eng. Comput.,* vol. 54, no. 11, pp. 1683-1694, 2016.
[http://dx.doi.org/10.1007/s11517-016-1458-0] [PMID: 26906280]

[33]   F.M. Susin, S. Espa, R. Toninato, S. Fortini, and G. Querzoli, "Integrated strategy for *in vitro* characterization of a bileaflet mechanical aortic valve", *Biomed. Eng. Online,* vol. 16, no. 1, p. 29,

2017.
[http://dx.doi.org/10.1186/s12938-017-0314-2] [PMID: 28209171]

[34] C.G. DeGroff, R. Shandas, and L. Valdes-Cruz, "Analysis of the effect of flow rate on the Doppler continuity equation for stenotic orifice area calculations: A numerical study", *Circulation,* vol. 97, no. 16, pp. 1597-1605, 1998.
[http://dx.doi.org/10.1161/01.CIR.97.16.1597] [PMID: 9593565]

[35] D. Garcia, P. Pibarot, J.G. Dumesnil, F. Sakr, and L-G. Durand, "Assessment of aortic valve stenosis severity: A new index based on the energy loss concept", *Circulation,* vol. 101, no. 7, pp. 765-771, 2000.
[http://dx.doi.org/10.1161/01.CIR.101.7.765] [PMID: 10683350]

[36] A.E. Weyman, and M. Scherrer-Crosbie, "Aortic stenosis: physics and physiology--what do the numbers really mean?", *Rev. Cardiovasc. Med.,* vol. 6, no. 1, pp. 23-32, 2005.
[PMID: 15741922]

[37] H. Rouse, "Fluid mechanics for hydraulic engineers", *Organizat. Behav. Human Decis. Process,* vol. 50, no. 2, pp. 179-211, 1938.

[38] M. Weininger, F. Sagmeister, S. Herrmann, V. Lange, U.J. Schoepf, M. Beissert, W. Voelker, H. Koestler, D. Hahn, F. Weidemann, and M. Beer, "Hemodynamic assessment of severe aortic stenosis: MRI evaluation of dynamic changes of vena contracta", *Invest. Radiol.,* vol. 46, no. 1, pp. 1-10, 2011.
[http://dx.doi.org/10.1097/RLI.0b013e3181f79ca2] [PMID: 21102347]

[39] T. Hahn, A.P. Condurache, T. Aach, M. Scharfschwerdt, and M. Misfeld, Automatic *in-vitro* orifice area determination and fluttering analysis for tricuspid heart valves.*Bildverarbeitung für die Medizin 2006.,* Springer, 2006, pp. 21-25.
[http://dx.doi.org/10.1007/3-540-32137-3_5]

[40] D. Wendt, S. Stühle, P. Marx, J. Benedik, H. Wendt, T. Stühle, M. Thoenes, M. Thielmann, H. Jakob, and W. Kowalczyk, "The investigation of systolic and diastolic leaflet kinematics of bioprostheses with a new *in-vitro* test method", *Minim. Invasive Ther. Allied Technol.,* vol. 24, no. 5, pp. 274-281, 2015.
[PMID: 26358833]

[41] L.N. Scotten, and D.K. Walker, "New laboratory technique measures projected dynamic area of prosthetic heart valves", *J. Heart Valve Dis.,* vol. 13, no. 1, pp. 120-132, 2004.
[PMID: 14765850]

[42] I. Borazjani, and F. Sotiropoulos, "The effect of implantation orientation of a bileaflet mechanical heart valve on kinematics and hemodynamics in an anatomic aorta", *J. Biomech. Eng.,* vol. 132, no. 11, 2010.111005
[http://dx.doi.org/10.1115/1.4002491] [PMID: 21034146]

[43] Y. Dabiri, J. Ronsky, I. Ali, A. Basha, A. Bhanji, and K. Narine, "Effects of leaflet design on transvalvular gradients of bioprosthetic heart valves", *Cardiovasc. Eng. Technol.,* vol. 7, no. 4, pp. 363-373, 2016.
[http://dx.doi.org/10.1007/s13239-016-0279-5] [PMID: 27573761]

[44] B. Vennemann, T. Rösgen, P.P. Heinisch, and D. Obrist, "Leaflet kinematics of mechanical and bioprosthetic aortic valve prostheses", *ASAIO J.,* vol. 64, no. 5, pp. 651-661, 2018.
[http://dx.doi.org/10.1097/MAT.0000000000000687] [PMID: 29045279]

[45] M.C. Wiggert, and D.C. Potter, *Mechanics of fluids.,* Brookes/Cole Thomson Learning: Pacific Grove, CA, 2002.

[46] M. Marriott, *Civil engineering hydraulics.,* John Wiley & Sons, 2009.

[47] R. Van Loon, "Towards computational modelling of aortic stenosis", *Int. J. Numer. Methods Biomed. Eng.,* vol. 26, no. 3–4, pp. 405-420, 2010.
[http://dx.doi.org/10.1002/cnm.1270]

[48] J. Garcia, P. Pibarot, R. Capoulade, F. Le Ven, L. Kadem, and É. Larose, "Usefulness of cardiovascular magnetic resonance imaging for the evaluation of valve opening and closing kinetics in aortic stenosis", *Eur Heart J Cardiovasc Imaging,* vol. 14, no. 18, pp. 819-826, 2013.
[http://dx.doi.org/10.1093/ehjci/jes314]

[49] D. Garcia, and L. Kadem, "What do you mean by aortic valve area: geometric orifice area, effective orifice area, or gorlin area?", *J. Heart Valve Dis.,* vol. 15, no. 5, pp. 601-608, 2006.
[PMID: 17044363]